Springer

KSME

Journal of Mechanical Science and Technology 26 (4) (2012) 1115~1126
www.springerlink.com/content/1738-494x
DOI 10.1007/s12206-012-0227-8

Efficient frequency response and its direct sensitivity analyses for large-size finite element models using Krylov subspace-based model order reduction †

Jeong Sam Han*

Department of Mechanical Design Engineering, Andong National University, Andong, 760-749, Korea

(Manuscript Received July 18, 2011; Revised December 1, 2011; Accepted January 18, 2012)

Abstract

In this paper, we examine an efficient calculation of the approximate frequency response (FR) for large-size finite element (FE) models using the Krylov subspace-based model order reduction (MOR) and its direct design sensitivity analysis with respect to design variables for sizing. Information about both the FR and its design sensitivity is necessary for typical gradient-based optimization iterations; therefore, the problem of high computational cost may occur when FRs of a large-size FE models are involved in the optimization problem. In the method suggested in this paper, reduced order models, generated from the original full-order FE models through the Arnoldi process, are used to calculate both the FR and FR sensitivity. This maximizes the speed of numerical computation of the FR and its design sensitivity. Assuming that the Krylov basis vectors remain constant with respect to the perturbation of a design variable, the FR sensitivity analysis is performed in a more efficient manner. As numerical examples, a car body with 535,992 degrees of freedom (DOF) and a 6 × 6 micro-resonator array with 368,424 DOF are adopted to demonstrate the numerical accuracy and efficiency of the suggested approach. Using the reduced-order models, we found that the FR and FR sensitivity are in a good agreement with those using the full-order FE model. The reduction in computation time is also found to be significant because of the use of Krylov subspace-based reduced models.

Keywords: Model order reduction; Frequency response; Direct design sensitivity analysis; Krylov subspace; Moment-matching method; Semi-analytical method; Car body; Micro-resonator array; Size optimization

1. Introduction

The frequency response (FR) of a structure and an FR design sensitivity analysis have been widely used for updating of finite element (FE) models, structural damage detection, structural dynamic optimization, vibration control, and so on because they have even more practical applications than the responses by eigenvalue analysis [1-6]. Generally, the FR of a structure is computed either by the direct method or by the mode superposition method (MSM). Although the direct method yields an exact solution, this method becomes computationally prohibitive when many excitation frequencies are involved and the dimensions of the system are large. On the other hand, the MSM is the most widely adopted to approximate FRs. The accuracy of the approximate FR is normally determined by how many relevant modal vectors are included to form a basis for approximating FRs. Therefore, using the MSM may also be cost-prohibitive for large-scale systems in terms of calculating the necessary eigenmodes with satisfactory accuracy. This drawback can be overcome to some extent through the use of modal truncation schemes that reduce the number of retained eigenmodes. However, the truncated errors of the FR obtained from the MSM with a modal truncation scheme can sometimes be very large. Therefore, improved variants to the MSM, such as the modal acceleration method, have been suggested to address the accuracy issue [1-5].

As relatively recent interests in this area, substructuring-based model reductions have been developed to improve efficiency in approximate FR analysis of large-scale systems. Automatic multilevel substructuring [7], substructuring reduction for the iteratively improved reduced system [8], fast frequency response analysis [9], algebraic substructuring [10], and combination of a subdomain method and a reduction method [11, 12] are included in this category. A variant of algebraic substructuring using the MSM enhanced by the so-called frequency sweep algorithm has recently been reported to obtain FRs near an extremely high-frequency range of interest [13].

In general, structural optimization involves a process of repeated simulation, by adjusting the design variables in an attempt to reach a design goal in which an objective function is minimized subject to a set of constraints. In order to make the correct modification, the rates of change in performance with

*Corresponding author. Tel.: +82 54 820 6218, Fax.: +82 54 820 5167
E-mail address: jshan@andong.ac.kr
† Recommended by Associate Editor Maenghyo Cho

respect to each design variable, that is, design sensitivities, should be provided. When the FR of a large-scale FE model is involved in gradient-based optimization iterations, the high computational cost required to calculate repeated FRs and their FR sensitivities in the optimization often becomes a hindrance in practical applications [14]. Therefore, it is necessary to find a solution in order to reduce the computation time in the FR and FR sensitivity during design optimization iterations.

Conventionally, the design sensitivity of a structural frequency response is calculated by either the direct method or the MSM. By differentiating the two types of FR equations, it is possible to produce two kinds of sensitivity formulations: direct formulations and mode superposition formulations. The former is based on the direct FR solution and results in an exact calculation of FR sensitivities for all cases permitted by the analytical formulation. On the other hand, the latter formulation has been the most widely adopted method for approximating FR sensitivities. However, it requires the calculation of the derivative of eigenvectors, which may sometimes be cost-prohibitive for large-scale models. Furthermore, for a system in which repeated modes exist among the active modes, the MSM may fail to obtain accurate results [5]. As an adaptive approach, Qu [4] proposed the MSM and mode acceleration method to calculate the approximate FR and its sensitivity according to the types of mode truncation. As a different approach, in early 1990s, a continuum design sensitivity analysis of the FR was developed [15] using the adjoint variable method. The reduced system generated by two-level condensation scheme (TLCS) was used to calculate semi-analytical sensitivity [16]. It should be noted here that the literature on FR sensitivity analysis contains information on the application of approximation methods to small FE models that, in many cases, do not actually require reduction.

In this paper, an efficient method that utilizes the Krylov subspace-based model order reduction (MOR) [6, 14, 17-22] is studied in order to calculate the approximation of both the FR and FR sensitivity with respect to sizing design variables over an entire frequency range of interest. The key idea herein is that equations of motion are reduced using a projection matrix generated from Krylov basis vectors instead of the traditional eigenvectors; then, direct FR and its sensitivity analyses are performed semi-analytically. The Krylov basis vectors are generated by the block-Arnoldi algorithm [17, 19] that comprises a series of static solutions; therefore, the computational costs are significantly lower compared to when normal eigenmodes are used [20].

The remainder of the paper is organized as follows. In section 2, we briefly review the conventional direct FR and FR sensitivity methods for a second-order system and explain the proposed method. In section 3, to verify the validity of the proposed method, we use the examples of a car body and a 6 × 6 micro-resonator array to report numerical results of the FR and FR sensitivities. Computational costs between the full-order model (FOM) and the reduced-order models (ROMs) are also compared and discussed. Finally, some concluding remarks are made in section 4.

2. Frequency response and its design sensitivity analyses

2.1 Frequency response analysis of a second-order system

The general form of the dynamic equations of motion for a damped system is given by a second-order system of ordinary differential equations (ODEs) in time:

$$\begin{aligned} \mathbf{M}\ddot{\mathbf{x}}(t) + \mathbf{C}\dot{\mathbf{x}}(t) + \mathbf{K}\mathbf{x}(t) &= \mathbf{F}(t) \\ \mathbf{y}(t) &= \mathbf{L}\mathbf{x}(t) \end{aligned} \tag{1}$$

where $\mathbf{M}$, $\mathbf{C}$, and $\mathbf{K} \in \Re^{N \times N}$ are the mass, damping, and stiffness matrices of the structure, respectively. The vectors $\ddot{\mathbf{x}}(t)$, $\dot{\mathbf{x}}(t)$, and $\mathbf{x}(t)$ present the acceleration, velocity, and displacement response vectors, respectively, and their dimensions are N. $\mathbf{F}(t)$ is the vector of applied forces, and $\mathbf{y}(t) \in \Re^{p}$ is the output measurement vector transformed from $\mathbf{x}(t)$ by $\mathbf{L} \in \Re^{p \times N}$, which is an output measurement matrix used to observe the response at certain points.

The corresponding dynamic equation of the structural system associated with harmonic excitation can be generally expressed in matrix form as

$$(-\Omega^2\mathbf{M} + i\Omega\mathbf{C} + \mathbf{K})\mathbf{x}(\Omega) = \mathbf{F}(\Omega) \tag{2}$$

where Ω is the circular frequency of excitation forces, and the response vector $\mathbf{x}(\Omega)$ is calculated using complex algebra pertaining to the excitation force vector $\mathbf{F}(\Omega)$ at a number of excitation frequencies over a frequency range of interest. Usually, the matrix $(-\Omega^2\mathbf{M} + i\Omega\mathbf{C} + \mathbf{K})$ is referred to as the dynamic stiffness matrix.

Conventionally, the FR of a system described in Eq. (2) is computed by either the direct method or the MSM. Formulations of FR sensitivity have been suggested by differentiating the two types of FR equations. Although the direct method yields the exact solution to Eq. (2), it becomes computationally prohibitive when many excitation frequencies are involved and the dimension of the system is large. On the other hand, the MSM has conventionally been the most widely adopted method for approximating FRs and their sensitivities. However, this method requires the calculation of the derivative of eigenvectors, which may sometimes be cost-prohibitive for large-scale systems. Furthermore, this method may not yield the correct result for a system wherein repeated modes exist among the active modes [5].

By taking the first partial derivative of the governing Eq. (2) with respect to a chosen design variable b_j (j = 1, 2, …, J), it is possible to obtain the direct FR sensitivities as follows:

$$\begin{aligned} &(-\Omega^2\mathbf{M} + i\Omega\mathbf{C} + \mathbf{K})\frac{\partial \mathbf{x}}{\partial b_j} \\ &= \frac{\partial \mathbf{F}}{\partial b_j} - \left(-\Omega^2 \frac{\partial \mathbf{M}}{\partial b_j} + i\Omega \frac{\partial \mathbf{C}}{\partial b_j} + \frac{\partial \mathbf{K}}{\partial b_j} \right)\mathbf{x} . \end{aligned} \tag{3}$$

Further, the sensitivity of the output measurement vector is derived from $\mathbf{y} = \mathbf{L}\mathbf{x}$ as

$$\frac{\partial \mathbf{y}}{\partial b_j} = \mathbf{L}\frac{\partial \mathbf{x}}{\partial b_j}. \tag{4}$$

Because the direct approach in Eqs. (2) and (3) provides the exact solution of the numerical models, the direct solution will be referenced when validating the proposed method. On the other hand, in the MSM, the sensitivities are obtained by differentiating the frequency responses that are expressed in a mode superposition form. This method necessitates s set of eigenvectors and their sensitivities. Qu [3] has discussed the advantages and disadvantages of these methods when used to calculate the FR and FR sensitivities.

The numerical cost of FR analysis is high for the following reasons: (1) the cost of solving the system of equations at each frequency can be tremendous and it increases significantly with an increase in the mesh density and complexity of the model; (2) many realistic problems require that the solution be evaluated for many individual frequencies. Therefore, when an accurate FR has to be obtained for large-frequency intervals, the computational load becomes so high that the calculation cannot be realistically performed in an industrial framework.

2.2 Frequency response analysis using Krylov subspace-based model order reduction

The basic idea of the Krylov subspace-based MOR is to find a low-dimensional subspace $\mathbf{V} \in \Re^{N\times n}$ of

$$\mathbf{x} \cong \mathbf{V}\mathbf{z} \quad \text{where } \mathbf{z} \in \Re^n,\ n << N \tag{5}$$

such that the trajectory of the original high-dimensional state vector $\mathbf{x}$ in Eq. (1) can be well approximated by the projection matrix $\mathbf{V}$ in relation to a considerably reduced vector $\mathbf{z}$ of order n. Implicit moment-matching through the Arnoldi process is the most efficient way to compute a reasonably accurate subspace $\mathbf{V}$ [17-19]. Provided that the subspace $\mathbf{V}$ is found, the original Eq. (1) is projected onto it. Multiplying the result by $\mathbf{V}^{\mathrm{T}}$ yields the following reduced system:

$$\begin{aligned} \mathbf{M}_{\mathrm{r}}\ddot{\mathbf{z}}(t) + \mathbf{C}_{\mathrm{r}}\dot{\mathbf{z}}(t) + \mathbf{K}_{\mathrm{r}}\mathbf{z}(t) &= \mathbf{F}_{\mathrm{r}}(t) \\ \mathbf{y}(t) &= \mathbf{L}_{\mathrm{r}}\mathbf{z}(t) \end{aligned} \tag{6}$$

where the subscript r denotes the reduced system matrix and $\mathbf{M}_{\mathrm{r}} = \mathbf{V}^{\mathrm{T}}\mathbf{M}\mathbf{V}$, $\mathbf{C}_{\mathrm{r}} = \mathbf{V}^{\mathrm{T}}\mathbf{C}\mathbf{V}$, $\mathbf{K}_{\mathrm{r}} = \mathbf{V}^{\mathrm{T}}\mathbf{K}\mathbf{V}$, $\mathbf{F}_{\mathrm{r}} = \mathbf{V}^{\mathrm{T}}\mathbf{F}$ and $\mathbf{L}_{\mathrm{r}} = \mathbf{L}\mathbf{V}$. The corresponding reduced system for Eq. (2) is given by

$$\begin{aligned} &(-\Omega^2\mathbf{M}_{\mathrm{r}} + i\Omega\mathbf{C}_{\mathrm{r}} + \mathbf{K}_{\mathrm{r}})\mathbf{z} = \mathbf{F}_{\mathrm{r}} \\ &\mathbf{y} = \mathbf{L}_{\mathrm{r}}\mathbf{z}\,. \end{aligned} \tag{7}$$

In terms of the moment-matching method for a proportionally damped structural dynamic system, it is shown that if the projection matrix $\mathbf{V}$ is chosen from a Krylov subspace of dimension n,

$$\begin{aligned} &\mathrm{colspan}\{\mathbf{V}\} = \Im_n(-\mathbf{K}^{-1}\mathbf{M}, \mathbf{K}^{-1}\mathbf{F}) \\ &= \mathrm{span}\{\mathbf{K}^{-1}\mathbf{F}, (-\mathbf{K}^{-1}\mathbf{M})\mathbf{K}^{-1}\mathbf{F}, \cdots, (-\mathbf{K}^{-1}\mathbf{M})^{n-1}\mathbf{K}^{-1}\mathbf{F}\}\,. \end{aligned} \tag{8}$$

The reduced system in Eq. (6) matches the first n moments of the full-order system [21]. Note that the reduction in the dimension of the original full-size system to $n << N$ is achieved; thus, FRs can be very efficiently calculated using Eq. (7). When a non-zero expansion point is adopted to obtain the projection matrix $\mathbf{V}$ in Eq. (8), the following relation is used:

$$\mathrm{colspan}\{\mathbf{V}\} = \Im_n\{(s_0\mathbf{M} + \mathbf{K})^{-1}\mathbf{M}, (s_0\mathbf{M} + \mathbf{K})^{-1}\mathbf{F}\} \tag{9}$$

where the expansion point is given by $s_0 = -(2\pi f_0)^2$, and the shift frequency f_0 is given in Hz.

2.3 Frequency response sensitivity analysis using Krylov subspace-based model order reduction

The direct method for the FR sensitivity analysis using the Krylov subspace-based MOR is derived by differentiating Eq. (7) with respect to design variable b_j; this yields

$$\begin{aligned} &(-\Omega^2\mathbf{M}_{\mathrm{r}} + i\Omega\mathbf{C}_{\mathrm{r}} + \mathbf{K}_{\mathrm{r}})\frac{\partial \mathbf{z}}{\partial b_j} \\ &= \frac{\partial \mathbf{F}_{\mathrm{r}}}{\partial b_j} - \left(-\Omega^2\frac{\partial \mathbf{M}_{\mathrm{r}}}{\partial b_j} + i\Omega\frac{\partial \mathbf{C}_{\mathrm{r}}}{\partial b_j} + \frac{\partial \mathbf{K}_{\mathrm{r}}}{\partial b_j}\right)\mathbf{z} \end{aligned} \tag{10}$$

where the calculation of the derivatives of $\mathbf{F}_{\mathrm{r}}$, $\mathbf{M}_{\mathrm{r}}$, $\mathbf{C}_{\mathrm{r}}$, and $\mathbf{K}_{\mathrm{r}}$ is necessary to form the right-hand side of the equation. By assuming that the projection matrix $\mathbf{V}$ in Eq. (5) can be treated as constant with respect to the perturbation of a design variable, that is, $\partial\mathbf{V}/\partial b_j = \mathbf{0}$, the first derivative of Eq. (5) becomes

$$\frac{\partial \mathbf{x}}{\partial b_j} = \frac{\partial \mathbf{V}}{\partial b_j}\mathbf{z} + \mathbf{V}\frac{\partial \mathbf{z}}{\partial b_j} \quad \rightarrow \quad \frac{\partial \mathbf{x}}{\partial b_j} = \mathbf{V}\frac{\partial \mathbf{z}}{\partial b_j} \tag{11}$$

and the derivatives of $\mathbf{F}_{\mathrm{r}}$, $\mathbf{M}_{\mathrm{r}}$, $\mathbf{C}_{\mathrm{r}}$, and $\mathbf{K}_{\mathrm{r}}$ can be expressed by

$$\begin{aligned} \frac{\partial \mathbf{F}_{\mathrm{r}}}{\partial b_j} &= \mathbf{V}^{\mathrm{T}}\frac{\partial \mathbf{F}}{\partial b_j} \\ \frac{\partial \mathbf{M}_{\mathrm{r}}}{\partial b_j} &= \mathbf{V}^{\mathrm{T}}\frac{\partial \mathbf{M}}{\partial b_j}\mathbf{V} \\ \frac{\partial \mathbf{C}_{\mathrm{r}}}{\partial b_j} &= \mathbf{V}^{\mathrm{T}}\frac{\partial \mathbf{C}}{\partial b_j}\mathbf{V} \\ \frac{\partial \mathbf{K}_{\mathrm{r}}}{\partial b_j} &= \mathbf{V}^{\mathrm{T}}\frac{\partial \mathbf{K}}{\partial b_j}\mathbf{V}\,, \end{aligned} \tag{12}$$

respectively. By substituting in Eq. (10), the FR sensitivity

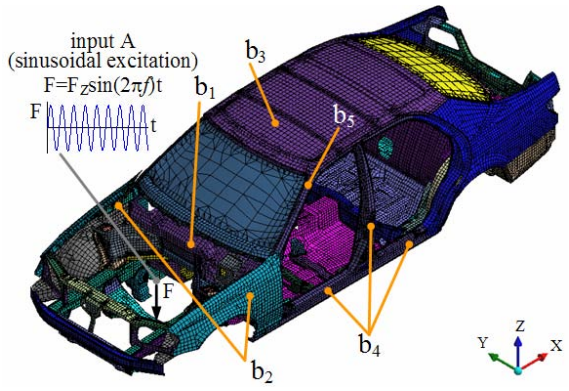

Fig. 1. The finite element model of a car body.

equation can be rewritten as

$$(-\Omega^2\mathbf{M}_r + i\Omega\mathbf{C}_r + \mathbf{K}_r)\frac{\partial \mathbf{z}}{\partial b_j} = \mathbf{V}^T\left(\frac{\partial \mathbf{F}}{\partial b_j} - \left(-\Omega^2\frac{\partial \mathbf{M}}{\partial b_j} + i\Omega\frac{\partial \mathbf{C}}{\partial b_j} + \frac{\partial \mathbf{K}}{\partial b_j}\right)\mathbf{V}\mathbf{z}\right). \quad (13)$$

Then, the derivative of output measurement vector with respect to the design variable is expressed by

$$\frac{\partial \mathbf{y}}{\partial b_j} = \mathbf{L}\mathbf{V}\frac{\partial \mathbf{z}}{\partial b_j}. \quad (14)$$

A similar assumption for the sensitivity of a modal matrix is sometimes used to avoid computing the sensitivities of the eigenvectors. The issue of whether to differentiate the basis vectors from eigenmodes or treat them as constants was discussed by Greene and Haftka [23] in terms of accuracy and cost tradeoffs.

3. Numerical examples

3.1 Car body

In order to demonstrate the numerical accuracy and efficiency of this method, we use the example of a car body [24], shown in Fig. 1. The car body is discretized into 91,525 shell elements, 4,017 weld spots, and 362 mass elements through the commercial FE package ANSYS [25], and it has 93,349 nodes. Therefore, the total number of degrees of freedom (DOF) of the full-order FE model is up to 535,992. The Young's modulus E = 207 GPa, mass density ρ = 7800 kg/m^3, and Poisson's ratio υ = 0.28 are used for the shell elements. The various colors in Fig. 1 denote the differing thickness of each part. In this case, the car body consists of 111 panels with thickness varying between 0.7 and 4 mm.

A free-free boundary condition is assumed in this case. Structural damping with Rayleigh damping constants α = 2.09 s^{-1} and β = 0.106 ms are adopted for the FRs.

Table 1. First 50 natural frequencies of the car body.

Mode	Frequency (Hz)	Mode	Frequency (Hz)
1	11.868	26	30.485
2	14.328	27	31.115
3	14.772	28	31.243
4	16.139	29	31.547
5	17.273	30	31.990
6	18.122	31	32.133
7	18.461	32	32.347
8	19.641	33	32.708
9	19.938	34	32.944
10	20.513	35	33.999
11	20.721	36	34.430
12	21.379	37	34.923
13	22.161	38	35.348
14	22.447	39	35.691
15	23.245	40	35.923
16	23.656	41	36.431
17	25.300	42	37.186
18	25.786	43	37.469
19	26.241	44	37.648
20	26.618	45	38.470
21	27.256	46	38.611
22	28.057	47	38.884
23	28.311	48	39.060
24	29.424	49	39.156
25	29.883	50	39.246

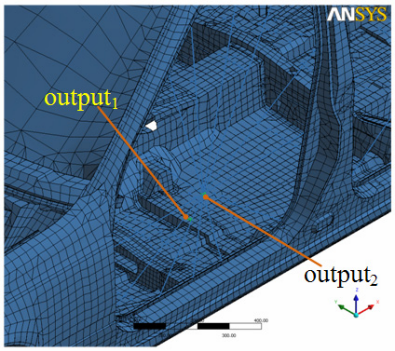

Fig. 2. Definition of output nodes for the response measurement.

3.1.1 Frequency response

A sinusoidal force of F_Z = 1 kN is applied in the z-direction to a mass element (input A) representing the engine of the car (see Fig. 1). The FRs are observed at input A and outputs 1 and 2. As shown in Fig. 2, the output points are located on the floor of the car body under the driver's seat (output$_1$) and at the master node that represents the mass center of the driver's door (output$_2$). The first 50 natural frequencies of the car body are listed in Table 1. Since the fundamental natural frequency exists around 12 Hz, and the responses above 50 Hz are al-

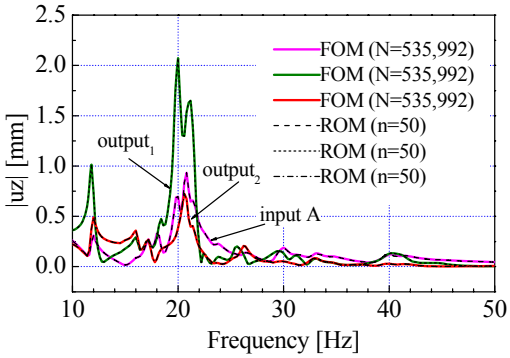

(a) Displacement in the z-direction (uz)

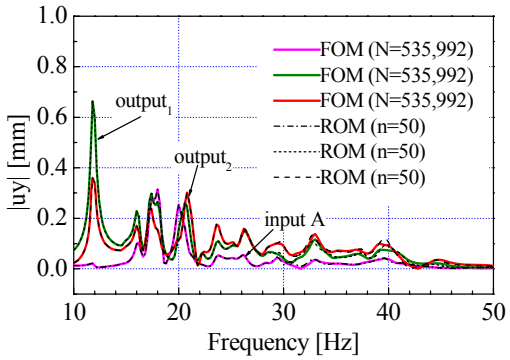

(b) Displacement in the y-direction (uy)

Fig. 3. Frequency responses from FOM and ROM (n = 50).

most negligible, the frequency range of interest for the excited force is selected between 10 and 50 Hz; further, a total of 200 frequency increments are evaluated over the range of interest. In fact, a frequency range below 100 Hz is considered as a low-frequency range for a car body, and a vibro-acoustic model can sometimes require a range up to about 800 Hz [26]. The frequency responses at input A and outputs 1 and 2 in the z- and y-direction are calculated for the FOM and some of the ROMs. Since the frequency range of interest is not from 0 Hz but from 10 Hz, the frequency shift f_0 = 10 Hz in Eq. (9) is adopted to make the dynamic stiffness matrix non-singular in this case. When the projection matrix is generated by the Arnoldi process [17-19], the system matrices are extracted directly from the ANSYS FE model.

In fact, the approximate FRs from this method are deemed to be extremely accurate so much so the results obtained by the FOM (N = 535,992) and ROM (n = 50) are indiscernible in the frequency range of interest (see Fig. 3). The peaks of observation points in the z-direction occur around 20 Hz, and among them, the amplitude of output 1 is about 2 mm, as shown in Fig. 4. On the other hand, the peaks of the output points in the y-direction are observed around 12 Hz. In both directions, the FRs are almost negligible above 50 Hz.

In order to check the accuracy of approximate FRs from ROMs, relative errors defined as Eq. (15) are plotted in Figs. 5 and 6.

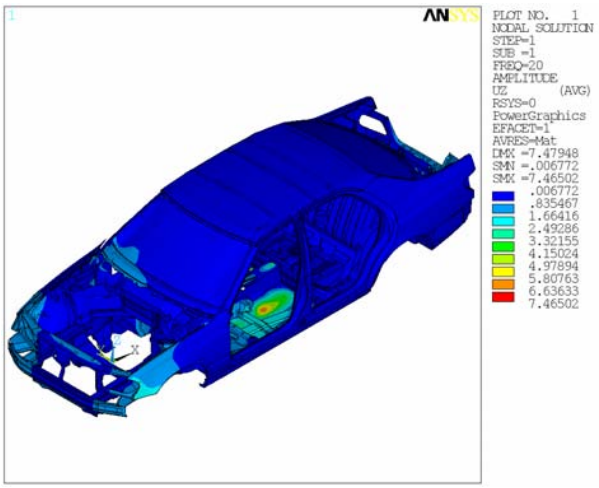

Fig. 4. Amplitude of frequency response in the z-direction at 20 Hz.

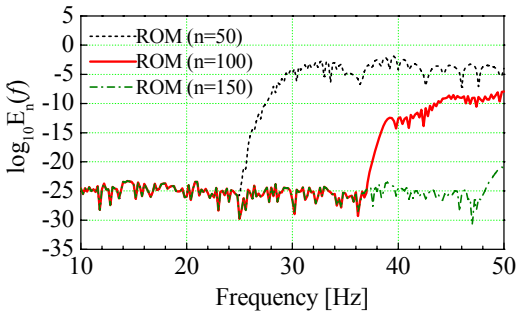

(a) uz at input A

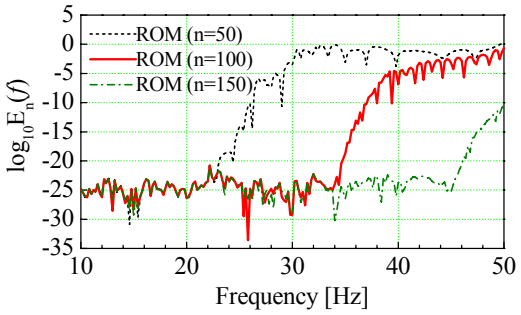

(b) uz at ouput 1

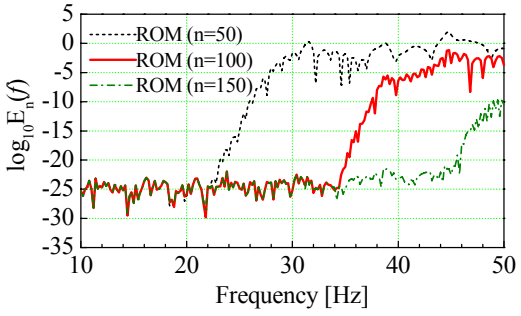

(c) uz at ouput 2

Fig. 5. Relative errors of frequency responses in the z-direction according to the order of reduced models.

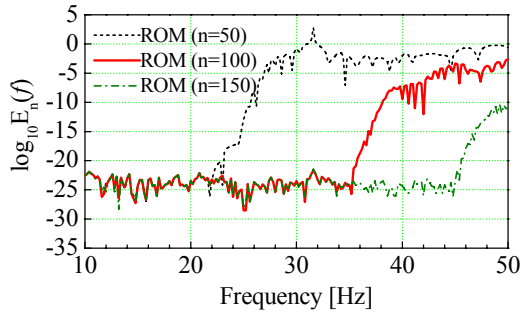

(a) uy at input A

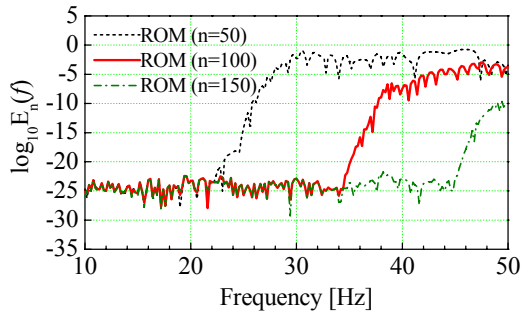

(b) uy at ouput 1

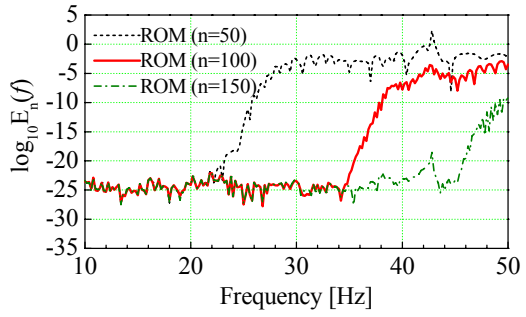

(c) uy at ouput 2

Fig. 6. Relative errors of frequency responses in the y-direction according to the order of reduced models.

$$E_n(f) = \frac{\left\| \hat{H}_n(f) - H(f) \right\|}{\left\| H(f) \right\|} \tag{15}$$

Here, $\hat{H}_n(f)$ and $H(f)$ refer to the FRs calculated from a ROM of order n and the FOM, respectively. Note that the relative errors are very small up to certain frequencies, but tend to increase abruptly at higher frequency ranges. It should also be noted that the ROMs with higher orders yield more accurate approximate FRs over a wider frequency range of interest. For the FR in the z-direction, ROMs of orders 50, 100, and 150 have relative errors less than 10^{-20} until approximately 22, 34, and 46 Hz, respectively. The FR in the y-direction shows a similar tendency.

3.1.2 Design sensitivity of frequency response

The thicknesses of 5 parts of the car body were selected as design variables: (1) the panel separating the engine room from the cabin; (2) both fenders of the car; (3) the roof of the car; (4) the center pillar assembly with side members around the doors; (5) the A-pillar part (see Fig. 1). The design sensitivities of FRs calculated by Eqs. (3) and (13) are compared in Figs. 7-9 according to the order of the ROMs. Since the derivatives of the system matrices in the equations are in general difficult to calculate, these derivatives are often replaced by finite difference approximations. Therefore, the combination of the direct FR sensitivity equations with finite difference matrix derivatives is known as a semi-analytical method [23]. The derivatives of the system matrices were approximated using the forward difference method with 0.1% design perturbations as follows:

$$\begin{aligned} \frac{\partial \mathbf{M}}{\partial b_j} &= \frac{\mathbf{M}(\mathbf{b} + \Delta b_j) - \mathbf{M}(\mathbf{b})}{\Delta b_j} \\ \frac{\partial \mathbf{C}}{\partial b_j} &= \frac{\mathbf{C}(\mathbf{b} + \Delta b_j) - \mathbf{C}(\mathbf{b})}{\Delta b_j} \\ \frac{\partial \mathbf{K}}{\partial b_j} &= \frac{\mathbf{K}(\mathbf{b} + \Delta b_j) - \mathbf{K}(\mathbf{b})}{\Delta b_j}. \end{aligned} \tag{16}$$

For simplicity, only the FRs in the z-direction are considered for FR sensitivity. In terms of the FRs in the z-direction, the design variables b_1 and b_4 have the two largest sensitivities. The FR is least sensitive to the thickness of the A-pillar part (b_5) (see Figs. 7-9). The accuracy of design sensitivities calculated from the ROM of order 50 is fairly good compared to the results obtained by the direct method using FOM. Therefore, the approximate FR sensitivities could be used for engineering purposes. The computed sensitivities from the ROM of order 150 perfectly match those obtained from FOM. On the other hand, the lower-order ROMs yield relatively accurate sensitivities, albeit with slight discrepancies at some frequencies. It is found that in the case of the ROM with n = 50, the accuracy of the FR sensitivities in Figs. 7-9 begins to decrease near 30 Hz.

This corresponds well to the frequency at which the relative errors in Fig. 5(a) become larger than roughly 10^{-5}. A similar tendency is found for the ROM with n = 100; the good agreement of FR sensitivity breaks around 40 Hz, where the relative errors exceeds 10^{-5} (see Fig. 5(b)). For the ROM with n = 150, the approximate FR sensitivities from this method are not distinguishable from those by FOM in the frequency range of interest (see Figs. 7-9).

Regarding the FR sensitivity analysis, both the force term and the dynamic stiffness matrix in Eq. (13) are approximated to calculate their derivatives; consequently, the accuracy of the FR sensitivity slightly decreases compared to that of only the FR. In other words, if the same number of Krylov vectors is adopted for calculating FRs and FR design sensitivities in the frequency range of interest, the errors in the former are generally smaller than those in the latter.

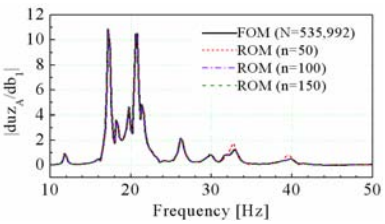

(a) uz at input A w.r.t. b_1

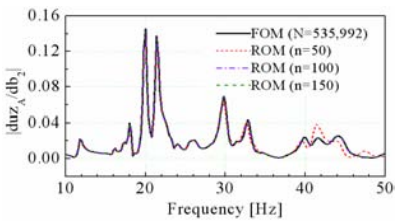

(b) uz at input A w.r.t. b_2

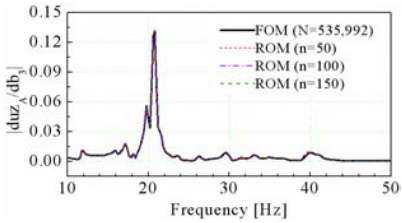

(c) uz at input A w.r.t. b_3

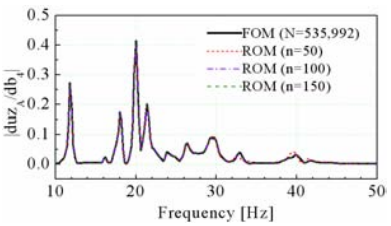

(d) uz at input A w.r.t. b_4

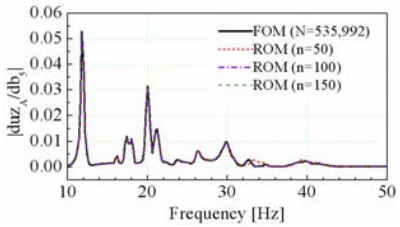

(e) uz at input A w.r.t. b_5

Fig. 7. Design sensitivities of the frequency responses at input A according to the order of reduced models.

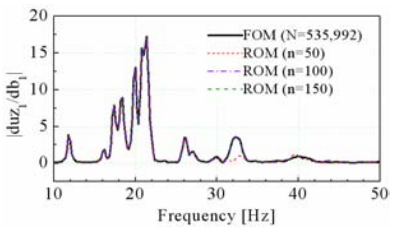

(a) uz at output 1 w.r.t. b_1

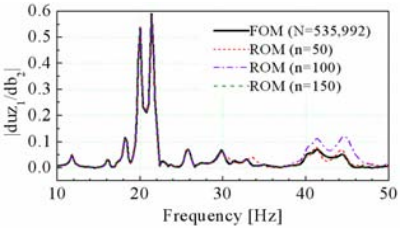

(b) uz at output 1 w.r.t. b_2

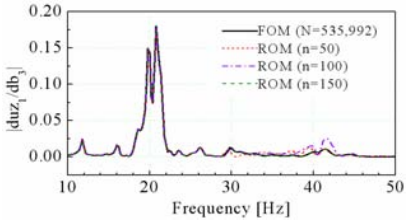

(c) uz at output 1 w.r.t. b_3

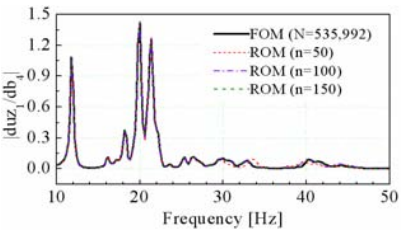

(d) uz at output 1 w.r.t. b_4

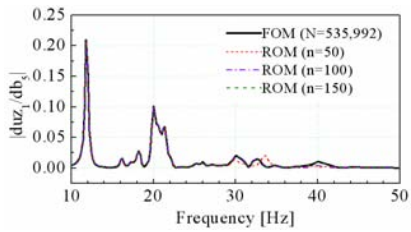

(e) uz at output 1 w.r.t. b_5

Fig. 8. Design sensitivities of the frequency responses at output 1 according to the order of reduced models.

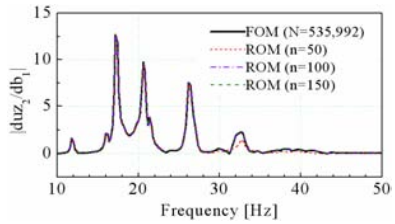

(a) uz at output 2 w.r.t. b_1

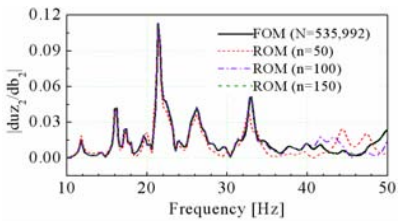

(b) uz at output 2 w.r.t. b_2

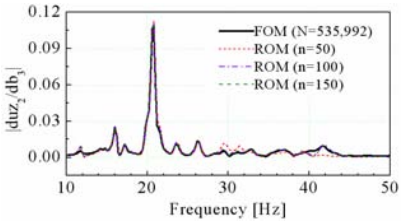

(c) uz at output 2 w.r.t. b_3

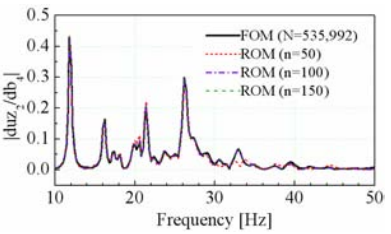

(d) uz at output 2 w.r.t. b_4

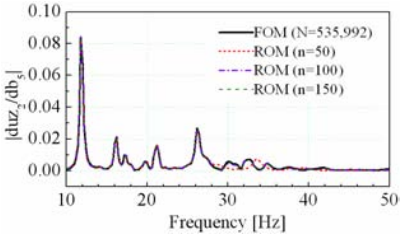

(e) uz at output 2 w.r.t. b_5

Fig. 9. Design sensitivities of the frequency responses at output 2 according to the order of reduced models.

3.2 6 ×6 micro-resonator array

As a second numerical example, we use a 6 × 6 micro-resonator array [13, 27], which utilizes the extensional wine-glass mode [28] in order to provide a high Q-factor (see Fig. 10). A filter with a micro-scale mechanical resonator can be integrated on a chip, thus decreasing insertion loss and improving battery life. An important factor in designing a filter is obtaining the desired FR within a specific range. One approach to obtaining an FR with the desired bandwidth in a high-frequency range is the construction of an array type from a single micro-resonator [28, 29]. Here, an FR between 634 and 638 MHz and its sensitivities are considered for the micro-resonator array.

The micro-resonator array is discretized into 57,600 shell elements and 1,008 beam elements through the commercial FE package ANSYS [25], and it has 61,428 nodes. Therefore, the total number of DOFs of the full-order FE model is up to 368,424. The structure is made of silicon; Young's modulus E = 150 GPa, mass density ρ = 2,300 kg/m^3, and Poisson's ratio υ = 0.226 are used for the FE model.

All beam-ends are clamped as a boundary condition. Structural damping with Rayleigh damping constants $\alpha = 428.9 \times 10^3$ s^{-1} and $\beta = 26.9 \times 10^{-15}$ s are adopted for the calculation of FRs.

3.2.1 Frequency response

An input force of F_R = 1 nN/μm is harmonically applied in the radial direction to the rings at the first column of the array, as shown in Fig. 10. All the middle points at the outer edge in the fourth quadrant of rings (1, 6)–(6, 6) are selected for output detection; thus, the amplitudes of radial displacement at each of the ELCs are observed as the FR. The frequency range of interest for the micro-resonator array is selected between 634 and 638 MHz; further, a total of 400 frequency increments are evaluated over the range of interest.

The FRs at ELC_4 and ELC_5 in the radial direction are calculated for the FOM and some of the ROMs. Since the frequency range of interest is between 634 and 638 MHz, the frequency shift f_0 = 636 MHz in Eq. (9) is adopted to make the projection matrix **V** more accurate in this frequency range. In fact, the approximate FRs from this method are deemed to be extremely accurate, so much so that the results obtained by the FOM (N = 368,424) and ROM (n = 100) are indiscernible in the frequency range of interest (see Fig. 11). The peaks of the observation points in the radial direction occur around 636 MHz, and correspond to the extensional wine-glass mode of rings (4, 6) and (5, 6) as shown in Fig. 12.

In order to check the accuracy of approximate FRs from ROMs, relative errors, given by Eq. (15), are plotted in Fig. 13. Note that the relative errors are minimal from the expansion point of 636 MHz to certain frequencies but tend to increase abruptly at higher frequency ranges. It should also be noted that the ROMs with higher orders yield more accurate approximate FRs over a wider frequency range of interest. For the FR at ELC_4, ROMs of orders 150 and higher have relative errors less than 10^{-12} over the entire frequency range of interest. The FR at ELC_5 shows a similar tendency.

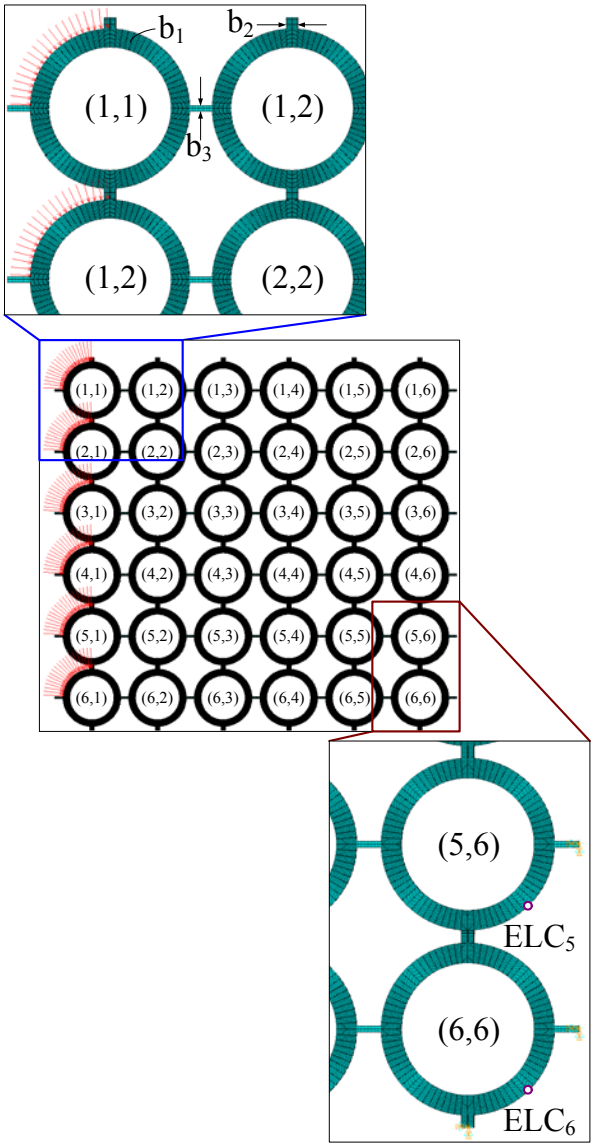

Fig. 10. The finite element model of a 6×6 micro-resonator array.

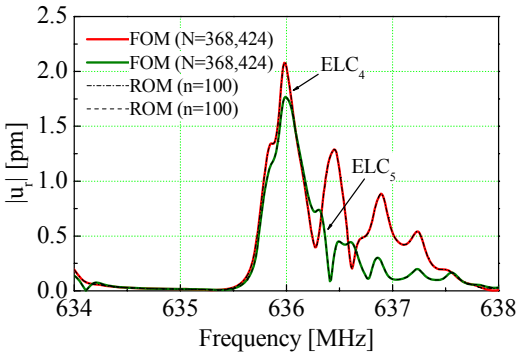

Fig. 11. Frequency responses from FOM and ROM (n = 100).

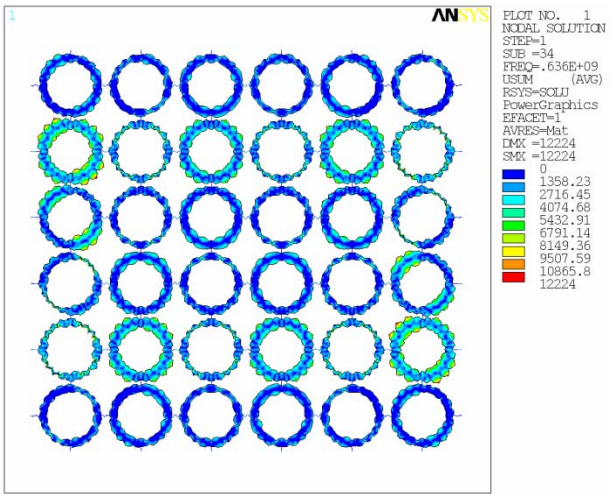

Fig. 12. Resonant mode shape close to the extensional wine-glass mode of rings (f = 636.035 MHz).

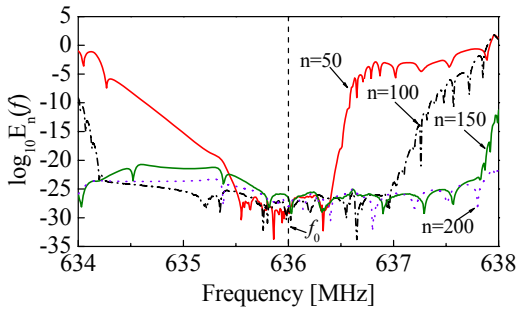

(a) ur at ELC_4

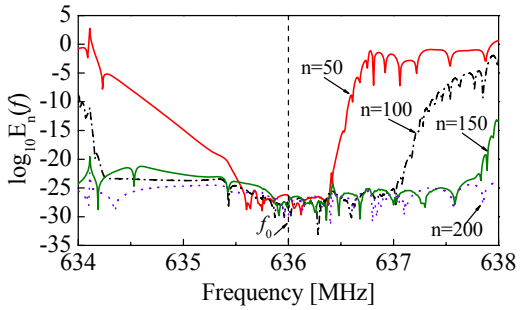

(b) ur at ELC_5

Fig. 13. Relative errors of frequency responses in the radial direction according to the order of reduced models.

3.2.2 Design sensitivity of frequency response

The thickness of rings (b_1), the width of strong vertical beams (b_2), and the width of weak horizontal beams (b_3) were selected as the design variables, as shown in Fig. 10. The design sensitivities of FRs calculated by Eqs. (3) and (13) are compared in Figs. 14 and 15 according to the order of the ROMs. The derivatives of the system matrices in the equations were calculated by Eq. (16) using the forward difference method with 0.1% design perturbations.

In terms of the FRs in the radial direction, the design variables b_2 and b_3 have larger sensitivities than b_1. Although there are slight discrepancies at some frequencies, the accuracy of the design sensitivities calculated from the ROM of order 50 is good compared to the results obtained by the direct method using FOM. It is also found that in this case, the accuracy of the FR sensitivities begins to decrease around 634 and 636.5 MHz (see Figs. 14 and 15). This corresponds well to the frequency at which the relative errors in Fig. 13 become larger than roughly 10^{-5}. The computed sensitivities from the ROMs of orders 100 and higher are not distinguishable from those by FOM in the frequency range of interest as shown in Figs. 14 and 15.

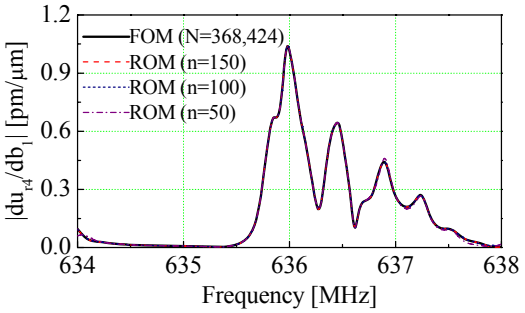

(a) ur at ELC_4 w.r.t. b_1

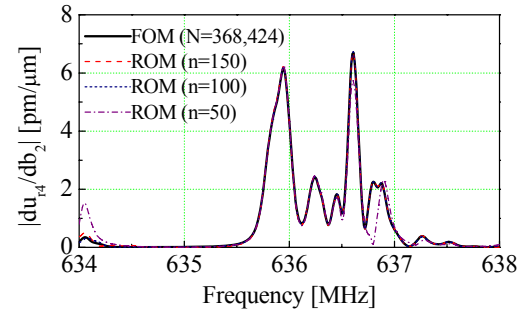

(b) ur at ELC_4 w.r.t. b_2

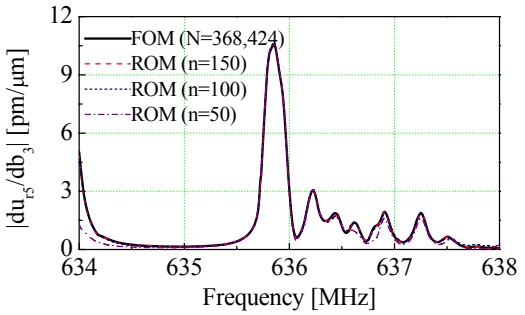

(c) ur at ELC_4 w.r.t. b_3

Fig. 14. Design sensitivities of the frequency responses at ELC_4 according to the order of reduced models.

3.3 Comparison of computation time

Thus far, we have demonstrated the numerical accuracy of approximate FRs and FR sensitivities through the application

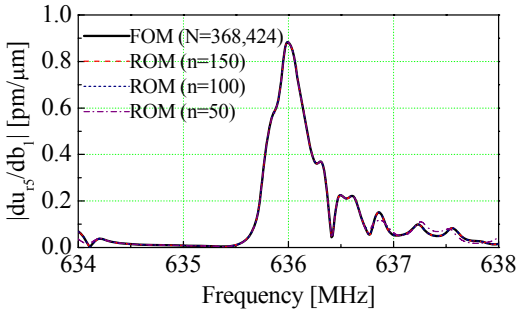

(a) ur at ELC_5 w.r.t. b_1

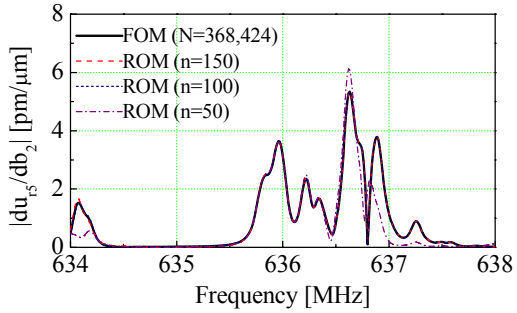

(b) ur at ELC_5 w.r.t. b_2

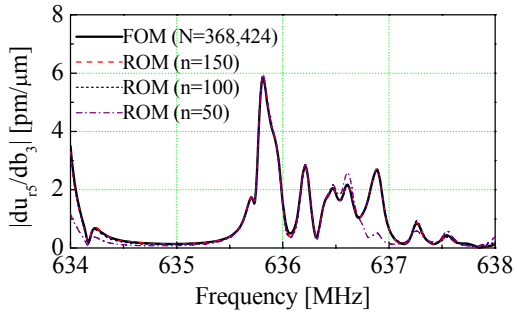

(c) ur at ELC_5 w.r.t. b_3

Fig. 15. Design sensitivities of the frequency responses at ELC_5 according to the order of reduced models.

examples. In this section, we compare the efficiency of the computation times for FR and FR sensitivity. The calculations were performed using MATLAB [30] on an HP workstation xw8400 with dual Xeon 5160 processors and 16 GB RAM.

In the case of the car body, the FR calculation using FOM takes about 79,530 s. On the other hand, ROMs with n = 50, 100, and 150 have substantially reduced computational costs, that is, 0.23%, 0.43%, and 0.65% of that of the FOM, respectively. The computation time for FR sensitivity with respect to each design variable is roughly 155,000 s, whereas the ROM of order 150, for instance, takes approximately 508 s to generate the Krylov vectors **V** in Eq. (13) and 383 s to calculate FR sensitivity. The computational cost for calculating FR sensitivity is almost double that of the FR calculation because the FR sensitivity calculation needs the solution of state vector **x** in advance, as depicted in Eq. (3). FR sensitivity calculations from ROMs with n = 50, 100, and 150 also have substantially reduced computational costs, that is, 0.31%, 0.44%, and 0.62% of that of the FOM, respectively.

Table 2. Computation times in seconds for the FRs and their sensitivities in the case of car body.

	FOM	ROM		
		n=50	n=100	n=150
Total DOF	535,992	50	100	150
Generation of ROM	-	177	340	508
Calculation of FR	79,530	2.8	3.6	4.8
Calculation of FR sensitivity	155,450	301	337	383

Table 3. Computation times in seconds for the FRs and their sensitivities in the case of 6 × 6 micro-resonator array.

	FOM	ROM		
		n=50	n=100	n=150
Total DOF	368,424	50	100	150
Generation of ROM	-	62	120	181
Calculation of FR	18,923	2.5	9.4	21.5
Calculation of FR sensitivity	34,143	504	592	711

In the case of the micro-resonator array, the FR calculation using FOM takes about 18,923 s. On the other hand, ROMs with n = 50, 100, and 150 have substantially reduced computational costs, that is, 0.34%, 0.68%, and 1.07% of that of the FOM, respectively. The computation time for FR sensitivity with respect to each design variable is roughly 34,140 s, whereas the ROM of order 150, for instance, takes approximately 181 s to generate the Krylov vectors **V** and 711 s to calculate FR sensitivity. FR sensitivity calculations from ROMs with n = 50, 100, and 150 also have substantially reduced computational costs, that is, 1.66%, 2.08%, and 2.61% of that of the FOM, respectively.

There is a tremendous reduction in the computational costs for FR and FR sensitivity because of the use of ROMs. Note that the computation times in Tables 2 and 3 may vary slightly, depending on the configuration of the computer used for operation, such as the I/O rates of the hard disk drives and the number of processes.

4. Conclusions

By using the Krylov subspace-based MOR, it is possible to calculate with great computational efficiency the approximate FR and FR design sensitivities with respect to sizing design variables for large-size FE models. Consequently, by using the suggested method, it is possible to resolve the problem of high computational costs in gradient-based optimizations with the FR-based constraints for large-size systems. Concretely, the following conclusions can be drawn from this study:

(1) For a car body with 535,992 DOF, the FRs up to 50 Hz by a ROM of order 50 are visually almost indistinguishable from the exact FRs using the FOM. In the case of a 6 × 6 mi-

cro-resonator array with 368,424 DOF, the FRs between 634 and 638 MHz by a ROM of order 100 are visually almost indistinguishable from the exact FRs using the FOM.

(2) The assumption that the Krylov basis vectors are treated as constant with respect to the perturbation of a design variable seems feasible. With this assumption, the accuracy of FR sensitivities calculated from a ROM with n = 50 for the car body and n = 100 for the micro-resonator array is fairly good compared to the case using the FOM. However, if the same number of Krylov vectors is used to calculate both FR and FR design sensitivity, the errors of the former are usually smaller than those of the latter.

(3) The relative errors in FRs by the ROMs are minimal up to a certain frequency, but tend to increase suddenly at higher frequency ranges. It is also noted that ROMs of higher orders produce more accurate FRs over a wider frequency range of interest.

(4) The remarkable reduction in computation times is because of the use of the Krylov subspace-based MOR. For the car body, the ROMs with n = 50, 100, and 150 have substantially reduced computational costs for FR calculations, that is, 0.23%, 0.43%, and 0.65% of that of the FOM, respectively. In the case of the FR sensitivity calculations, the ROMs with n = 50, 100, and 150 also have substantially reduced computational costs, that is, 0.31%, 0.44%, and 0.62% of that of the FOM, respectively. For the micro-resonator array, the ROMs with n = 50, 100, and 150 have substantially reduced computational costs for FR calculations, that is, 0.34%, 0.68%, and 1.07% of that of the FOM, respectively. In the case of the FR sensitivity calculations, the ROMs with n = 50, 100, and 150 also have significantly reduced computational costs, that is, 1.66%, 2.08%, and 2.61% of that of the FOM, respectively.

(5) In general, it can be said that the calculation of Krylov basis vectors for the projection matrix is computationally less expensive than modal eigenmodes; therefore, the proposed method is more efficient than the MSM in approximating FR and FR sensitivity, provided that the same formulation is used.

Finally, the suggested method for the simple and efficient approximation of FR and FR sensitivity is also applicable to the transient response and its sensitivity analyses. These related studies are currently in progress.

Acknowledgment

The author acknowledges the support from Basic Science Research Program through the National Research Foundation of Korea (NRF) funded by the Ministry of Education, Science and Technology (2010-0028152).

References

[1] Z. Q. Qu, Hybrid expansion method for frequency responses and their sensitivities, part I: undamped systems, *Journal of Sound and Vibration*, 231 (1) (2000) 175-193.

[2] Z. Q. Qu and R. P. Selvam, Hybrid expansion method for frequency responses and their sensitivities, part II: viscously damped systems, *Journal of Sound and Vibration*, 238 (3) (2000) 369-388.

[3] Z. Q. Qu, Accurate methods for frequency responses and their sensitivities of proportionally damped systems, *Computers and Structures*, 79 (2001) 87-96.

[4] Z. Q. Qu, Adaptive mode superposition and acceleration technique with application to frequency response function and its sensitivity, *Mechanical Systems and Signal Processing*, 21 (1) (2007) 40-57.

[5] T. Ting, Design sensitivity analysis of structural frequency response, *AIAA Journal*, 31 (10) (1993) 1965-1967.

[6] J. S. Han, Direct design sensitivity analysis of frequency response function using Krylov subspace based model order reduction, *Journal of the Computational Structural Engineering Institute of Korea*, 23 (2) (2010) 153-163.

[7] J. K. Bennighof and M. F. Kaplan, Frequency sweep analysis using multi-level substructuring, global modes and iteration, *Proceedings of 39th AIAA/ASME/ASCE/AHS Structures*, Structural Dynamics and Materials Conference (1998).

[8] D. Choi, H. Kim and M. Cho, Improvement of substructuring reduction technique for large eigenproblems using an efficient dynamic condensation method, *Journal of Mechanical Science and Technology*, 22 (2) (2008) 255-268.

[9] C. W. Kim and J. K. Bennighof, Fast frequency response analysis of large-scale structures with non-proportional damping, *International Journal for Numerical Methods in Engineering*, 69 (5) (2006) 978-992.

[10] W. Gao, X. S. Li, C. Yang and Z. Bai, An implementation and evaluation of the AMLS method for sparse eigenvalue problems, *ACM Transactions on Mathematical Software*, 34 (4) (2008) 20:1-28.

[11] H. Kim and M. Cho, Subdomain optimization of multi-domain structure constructed by reduced system based on the primary degrees of freedom, *Finite Elements in Analysis and Design*, 43 (2007) 912-930.

[12] H. Kim, M. Cho, H. Kim and H. G. Choi, Efficient construction of a reduced system in multi-domain system with free subdomains, *Finite Elements in Analysis and Design*, 47 (2011) 1025-1035.

[13] J. H. Ko, D. Byun and J. S. Han, An efficient numerical solution for frequency response function of micromechanical resonator arrays, *Journal of Mechanical Science and Technology*, 23 (10) (2009) 2694-2702.

[14] J. S. Han, E. B. Rudnyi and J. G. Korvink, Efficient optimization of transient dynamic problems in MEMS devices using model order reduction, *Journal of Micromechanics and Microengineering*, 15 (4) (2005) 822-832.

[15] K. K. Choi and J. H. Lee, Sizing design sensitivity analysis of dynamic frequency response of vibrating structures, *Journal of Mechanical Design*, 114 (1) (1992) 166-173.

[16] H. Kim and M. Cho, Two-level scheme for selection of primary degrees of freedom and semi-analytic sensitivity based on the reduced system, *Computer Methods in Applied Mechanics and Engineering*, 195 (33-36) (2006) 4244-4268.

[17] R. W. Freund, Krylov-subspace methods for reduced-order modeling in circuit simulation, *J. Comput. Appl. Math.*, (123) (2000) 395-421.

[18] Z. Bai, Krylov subspace techniques for reduced-order modeling of large-scale dynamical systems, *Applied Numerical Mathematics*, (43) (2002) 9-44.

[19] E. Rudnyi and J. Korvink, Model order reduction for large scale engineering models developed in ANSYS, *Lecture Notes in Computer Science*, 3732 (2006) 349-356.

[20] J. S. Han, Efficient vibration simulation using model order reduction, *Transactions of the KSME A*, 30 (3) (2006) 310-317.

[21] R. Eid, B. Salimbahrami, B. Lohmann, E. Rudnyi and J. Korvink, Parametric order reduction of proportionally damped second-order systems, *Sensors and Materials*, 19 (3) (2007) 149-164.

[22] J. Choi, M. Cho and J. Rhim, Efficient prediction of the quality factors of micromechanical resonators, *Journal of Sound and Vibration*, 329 (1) (2009) 84-95.

[23] W. H. Greene and R. T. Haftka, Computational aspects of sensitivity calculations in transient structural analysis, *Computers & Structures*, 32 (2) (1989) 433-443.

[24] ANSYS, Inc., ANSYS Paramesh Training Manual, Release 3.0, Canonsburg (2004).

[25] ANSYS, Inc., Theory Reference for ANSYS and ANSYS Workbench, ANSYS Release 11.0, Canonsburg (2007).

[26] A. Kropp and D. Heiserer, Efficient broadband vibroacoustic analysis of passenger car bodies using an FE-based component mode synthesis approach, *Journal of Computational Acoustics*, 11 (2) (2003) 139-157.

[27] J. S. Han and J. H. Ko, Frequency response analysis of array-type MEMS resonators by model order reduction using Krylov subspace method, *Transactions of the KSME A*, 33 (9) (2009) 878-885.

[28] Y. Xie, S. S. Li, Y. W. Lin, Z. Ren and C. T. C. Nguyen, UHF micromechanical extensional wing-glass mode ring resonators, Technical digest, 2003 IEEE International electron devices meeting, Washington DC (2003).

[29] M. Shalaby, M. Abdelmoneum and K. Saitou, Design of spring coupling for high Q, high frequency MEMS filter, *Proceedings of 2006 ASME International Mechanical Engineering Congress and Exposition*, Chicago, Illinois, USA (2006).

[30] The MathWorks, Inc. MATLAB Getting Started Guide (2011).

Jeong Sam Han received his B.S. degree in Mechanical Engineering from Kyungpook National University, Korea, in 1995. He then went on to receive his M.S. and Ph.D. degrees from KAIST, Korea, in 1997 and 2003, respectively. Dr. Han is currently a professor at the Department of Mechanical Design Engineering at Andong National University in Andong, Korea. Prof. Han's research interests cover the areas of model order reduction, structural optimization, and MEMS simulation, etc.